Supplemental Material for: Dynamical Glass and Ergodization Times in Classical Josephson Junction Chains

Thudiyangal Mithun,[1] Carlo Danieli,[1] Yagmur Kati,[1,2] and Sergej Flach[1]

[1] *Center for Theoretical Physics of Complex Systems, Institute for Basic Science, Daejeon 34051, Korea*

[2] *Basic Science Program, Korea University of Science and Technology (UST), Daejeon 34113, Republic of Korea*

I. STATISTICAL ANALYSIS

The energy density h is calculated with the microcanonical partition function

$$Z = \int_{-\infty}^{\infty}\int_{-\pi}^{\pi}\prod_n dp_n dq_n e^{-\beta H} \tag{1}$$

as

$$h = -\frac{1}{N}\frac{\partial \ln(Z)}{\partial \beta} = \frac{1}{2\beta} + E_J\big(1 - \frac{I_1(\beta E_J)}{I_0(\beta E_J)}\big), \tag{2}$$

with average potential energy density

$$u = E_J\big(1 - \frac{I_1(\beta E_J)}{I_0(\beta E_J)}\big) \tag{3}$$

and average kinetic energy density

$$k = \frac{1}{2\beta}. \tag{4}$$

In terms of k we rewrite Eq. 2 as

$$h = k + E_J\left(1 - \frac{I_1(E_J/2k)}{I_0(E_J/2k)}\right). \tag{5}$$

II. INTEGRATION

We split Eq. 1 in the main text as

$$A = \sum_{n=1}^{N}\frac{p_n^2}{2}\ , \qquad B = E_J\sum_{n=1}^{N}(1-\cos(q_{n+1}-q_n))\ . \tag{6}$$

As discussed in [1], this separation leads to a symplectic integration scheme called SBAB_2, where

$$\begin{aligned} e^{\Delta t\mathcal{H}} &= e^{\Delta t(A+B)} \approx e^{d_1\Delta t L_B}e^{c_2\Delta t L_A}e^{d_2\Delta t L_B} \\ &\times e^{c_2\Delta t L_A}e^{d_1\Delta t L_B} \end{aligned} \tag{7}$$

where $d_1 = \frac{1}{6}$, $d_2 = \frac{2}{3}$, $c_2 = \frac{1}{2}$. The operators $e^{\Delta t L_A}$ and $e^{\Delta t L_B}$ which propagate the set of initial conditions (q_n, p_n) from Eq. (6) at the time t to the final values $(q_n^{'}, p_n^{'})$ at the time $t+\Delta t$ are

$$\begin{aligned} e^{\Delta t L_A} &: \begin{cases} q_n^{'} = q_n + p_n\Delta t \\ p_n^{'} = p_n \end{cases} \\ e^{\Delta t L_B} &: \begin{cases} q_n^{'} = q_n \\ p_n^{'} = p_n + E_J\big[\sin(q_{n+1}-q_n) + \sin(q_{n-1}-q_n)\big]\Delta t \end{cases} \end{aligned} \tag{8}$$

We then introduce a corrector $C = \{\{A,B\},B\}$. Following [1], this term applies

$$\mathrm{SBAB}_2 C = e^{-\frac{g}{2}\Delta t^3 L_C}\,\mathrm{SBAB}_2\, e^{-\frac{g}{2}\Delta t^3 L_C} \tag{9}$$

for $g = 1/72$. The corrector term is

$$\begin{aligned} C &= -\sum_{n=1}^{N}\frac{\partial\{A,B\}}{\partial p_n}\frac{\partial B}{\partial q_n} = \sum_{n=1}^{N}\left(\frac{\partial B}{\partial q_n}\right)^2 \\ &= E_J^2\sum_{n=1}^{N}\big[\sin(q_{n+1}-q_n) + \sin(q_{n-1}-q_n)\big]^2. \end{aligned} \tag{10}$$

The corrector operator C yields to the following resolvent operator

$$e^{tL_C} : \begin{cases} q_n^{'} = q_n \\ p_n^{'} = p_n + E_J^2\Big\{2\big[\sin(q_{n+1}-q_n) + \sin(q_{n-1}-q_n)\big]\cdot\big[\cos(q_{n+1}-q_n) + \cos(q_{n-1}-q_n)\big] \\ \qquad -2\big[\sin(q_{n+2}-q_{n+1}) + \sin(q_n - q_{n+1})\big]\cdot\cos(q_n - q_{n+1}) \\ \qquad -2\big[\sin(q_n - q_{n-1}) + \sin(q_{n-2}-q_{n-1})\big]\cdot\cos(q_n - q_{n-1})\Big\}\Delta t \end{cases}$$

III. CALCULATION OF MAXIMAL LCE : TANGENT MAP METHOD AND VARIATIONAL EQUATIONS

If the autonomous Hamiltonian has the form [1]

$$H(\vec{q},\vec{p}) = \sum_{n=1}^{N}\left[\frac{1}{2}\vec{p}_n^2 + V(\vec{q})\right], \tag{11}$$

the equations of motion are

$$\begin{bmatrix}\dot{\vec{q}} \\ \dot{\vec{p}}\end{bmatrix} = \begin{bmatrix}\vec{p} \\ -\frac{\partial V(\vec{q})}{\partial \vec{q}}\end{bmatrix} \tag{12}$$

The corresponding variational Hamiltonian and equations of motion are

$$H_V(\vec{\delta q}, \vec{\delta p}) = \sum_{n=1}^{N}\left[\frac{1}{2}\vec{\delta p}_n^2 + \frac{1}{2}\sum_{m=1}^{N} D_V^2(\vec{q})_{nm}\delta\vec{q}_n\delta\vec{q}_m\right], \tag{13}$$

$$\text{and} \quad \begin{bmatrix}\dot{\vec{\delta q}}\\ \dot{\vec{\delta p}}\end{bmatrix} = \begin{bmatrix}\vec{\delta p}\\ -D_V^2(\vec{q})\vec{\delta q}\end{bmatrix}, \tag{14}$$

respectively. Here,

$$D_V^2(q(\vec{t}))_{nm} = \frac{\partial^2 V(\vec{q})}{\partial\vec{q}_n\vec{q}_m}|_{\vec{q}(t)} \tag{15}$$

For Eq.(1) in the main text, the variational equations of motion are

$$\begin{bmatrix}\dot{\delta q_n}\\ \dot{\delta p_n}\end{bmatrix} = \begin{bmatrix}\delta p_n\\ -E_J\big[-\cos(q_n-q_{n-1})\delta q_{n-1} + (\cos(q_{n+1}-q_n)+\cos(q_n-q_{n-1}))\delta q_n - \cos(q_{n+1}-q_n)\delta q_{n+1}\big]\end{bmatrix}, \tag{16}$$

The corresponding operators are

$$\begin{aligned} e^{\Delta t L_{AV}} &: \begin{cases}\vec{\delta q}' = \vec{\delta q} + \vec{\delta p}\Delta t\\ \vec{\delta p}' = \vec{\delta p}\end{cases}\\ e^{\Delta t L_{BV}} &: \begin{cases}\vec{\delta q}' = \vec{\delta q}\\ \vec{\delta p}' = \vec{\delta p} - D_V^2(\vec{q})\vec{\delta q}\Delta t\end{cases}\end{aligned} \tag{17}$$

Following [1], the corrector operator C yields the following resolvent operator

$$e^{\Delta t L_C} : \begin{cases}\vec{\delta q}' = \vec{\delta q}\\ \vec{\delta p}' = \vec{\delta p} - D_C^2(\vec{q})\vec{\delta q}\Delta t.\end{cases} \tag{18}$$

Here $D_C^2(\vec{q}) = \frac{\partial^2 C}{\partial q_n \partial q_m}$ is the Hessian.

From Eq. 18, we get

$$e^{\Delta t L_C} : \begin{cases} \delta q_n' = \delta q_n\\ \delta p_n' = \delta p_n - E_J^2\Big\{\big[2\cos(q_{n-2}-q_{n-1})\cos(q_n-q_{n-1})\big]\delta q_{n-2}\\ \quad +\big[-2\cos(q_{n-1}-2q_n+q_{n+1}) - 4\cos(2(q_n-q_{n-1})) - 2\cos(q_{n-2}-2q_{n-1}+q_n)\big]\delta q_{n-1}\\ \quad +\big[4\cos(2(q_{n+1}-q_n)) + 4\cos(q_{n-1}-2q_n+q_{n+1}) + 4\cos(2(q_{n-1}-q_n)) - 2\sin(q_{n+2}-q_{n+1})\sin(q_n\\ \quad -q_{n+1}) - 2\sin(q_{n-2}-q_{n-1})\sin(q_n-q_{n-1})\big]\delta q_n\\ \quad +\big[-4\cos(2(q_{n+1}-q_n)) - 2\cos(q_{n-1}-2q_n+q_{n+1}) - 2\cos(q_{n+2}-2q_{n+1}+q_n)\big]\delta q_{n+1}\\ \quad +\big[2\cos(q_{n+2}-q_{n+1})\cos(q_n-q_{n+1})\big]\delta q_{n+2}\Big\}\Delta t \end{cases} \tag{19}$$

IV. NUMERICAL SIMULATION

We simulate Eqs. 2 in the main text with periodic boundary conditions $p_1 = p_{N+1}$ and $q_1 = q_{N+1}$ and time step $\Delta t = 0.1$. In the simulation, the relative energy error $\Delta E = |\frac{E(t)-E(0)}{E(0)}|$ is kept lower than 10^{-4}. The initial conditions follow by fixing the positions to zero $q_n = 0$ and by choosing the moments p_n according Maxwell's distribution. The total angular momentum $L = \sum_{n=1}^{N} p_n$ is set zero by a proper shift of all momenta $p_n - L/N$. Finally, we rescale $|p_n| \to a|p_n|$ to precisely hit the desired energy (density).

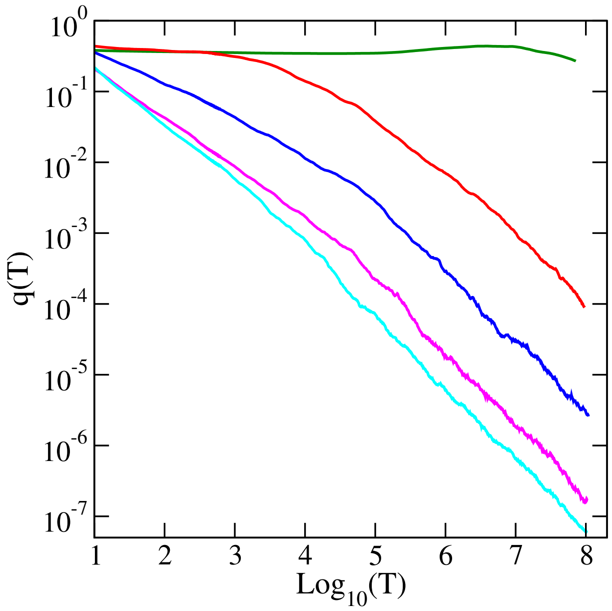

Figure 1: (Color online) Fluctuation index q for fixed the energy density $h = 1$ with $R = 12$. From top to bottom: $E_J = 0.1$ (green), $E_J = 0.5$ (red), $E_J = 1.0$ (blue), $E_J = 2.0$ (magenta) and $E_J = 3.0$ (cyan).

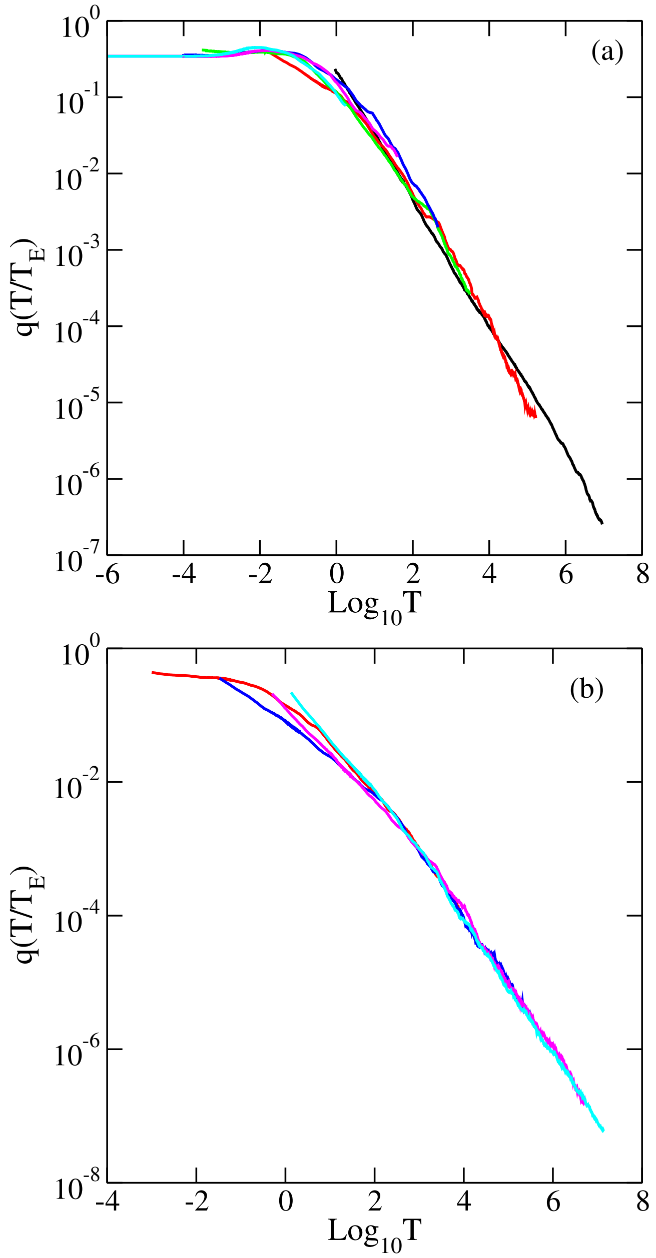

Figure 2: (Color online) a) $q(T/T_E)$ for fixed $E_J = 1$ with energy densities 0.1 (black) 1.2 (red), 2.4 (green), 3.8 (blue), 5.4 (magenta), and 8.5 (cyan) (corresponding to Fig. 1 in the main body); b) $q(T/T_E)$ for fixed energy density $h = 1$ with $E_J = 0.5$, (red), $E_J = 1.0$, (blue), $E_J = 2.0$, (magenta) and $E_J = 3.0$, (cyan) (corresponding to Fig. 1).

V. FINITE TIME AVERAGE FOR $h = 1$

Fig. 1 shows the index $q(T)$ for fixed energy $h = 1$ with varying coupling strengths, E_J. It is similar to Fig.1 from the main text for fixed E_J and varying h.

VI. EVALUATION OF THE ERGODIZATION TIME

We rescale and fit the fluctuation index $q(T)$ shown in Figs. 1 (main body) and 1 (in the supplement). We choose a parameter set with a clearly observed asymptotic $q(T) \approx T_E/T$ dependence, and fit this dependence to obtain T_E. We then rescale the variable $T \to xT$ for all other lines to obtain the best overlap with the initially chosen line as shown in Fig. 2. The scaling parameters x are then used to compute the corresponding ergodization times.

VII. ESTIMATE OF THE ERGODIZATION TIME T_E

In the main text, we defined the *ergodization time* T_E as the prefactor of the $1/T$ decay of the fluctuation index: $q(T \ll T_E) = q(0)$ and $q(T \gg T_E) \sim T_E/T$. We estimate this prefactor by approximating the time-dynamics of the observables $k_n(t)$ with telegraphic random process [2–4].

$$k_n(t) \approx \begin{cases} k + \alpha & \text{if } \; k_n(t) > k \\ k - \beta & \text{if } \; k_n(t) < k \end{cases} \tag{20}$$

with real constant α, β (for example see Fig. 4(a) of the main text, where $\alpha = 1 - k$ and $\beta = k$). This recast the finite time average $\overline{k}_{n,T} = \frac{1}{T}\int_0^T k_n(t)dt$ of k_n to

$$\begin{aligned} \overline{k}_{n,T} &\approx \frac{k+\alpha}{T}\sum_{i=1}^{M_n^+}\tau_n^+(i) + \frac{k-\beta}{T}\sum_{i=1}^{M_n^-}\tau_n^-(i) \\ &\equiv k + \frac{1}{T}\left[\alpha S_n^+ - \beta S_n^-\right] \end{aligned} \tag{21}$$

since $T = S_n^+ + S_n^-$. Here $M_n^\pm$ denote the number of excursions $\tau^\pm$ within a time interval $[0, T]$. As $\mu_k(T \to \infty) = k$ and $\sigma_k(T \to \infty) = 0$ (see main text), we focus only on the variance $\sigma_k(T)$ to estimate the dependence on T of the fluctuation index $q(T) = \frac{\sigma_k^2(T)}{\mu_k^2(T)}$. We first rewrite Eq.(21) in terms of S_n^+ only by adding and subtracting $\beta S_n^+/T$

$$\overline{k}_{n,T} \approx \frac{\alpha+\beta}{T}S_n^+ + k - \beta \tag{22}$$

By recalling that $\sigma_{k+B}^2(T) = \sigma_k^2(T)$ and $\sigma_{Bk}^2(T) = B^2\sigma_k^2(T)$ for any constant B, and by dropping the constant factor $(\alpha+\beta)$ it follows that $\sigma_k^2(T)$ scales as

$$\sigma_k^2(T) \sim \frac{1}{T^2}\sigma_{S_n^+}^2(T) \tag{23}$$

As the excursion times τ^+ are considered independent variables identically distributed, it follows that

$$\sigma_{S_n^+}^2(T) = M_n^+(T)\sigma_\tau^2 \tag{24}$$

with σ_τ^2 the variance of τ^+. For $T \gg \mu_\tau$ with μ_τ the first moment of τ^+, the number of events M_n^+ grows as $M_n^+ \sim T/\mu_\tau$. This yields

$$\sigma_k^2(T) \sim \frac{\sigma_\tau^2}{\mu_\tau}\frac{1}{T} \tag{25}$$

and ultimately to Eq. (4) of the main text.

VIII. LYAPUNOV EXPONENT COMPUTATION

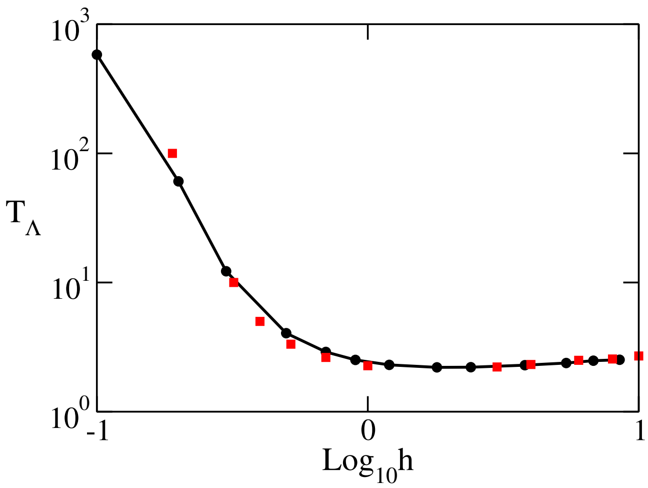

Figure 3: (Color online) Lyapunov time for fixed $E_J = 1$. The black circles represent our numerical results, and the red squares represent the analytical results from [5]. The black line guides the eye.

We compute the largest Lyapunov exponent Λ by numerically solving the variational equations

$$\dot{w}(t) = \left[J_{2N} \cdot D_H^2(x(t))\right] \cdot w(t) \tag{26}$$

for a small amplitude deviation $w(t) = (\gamma q(t), \gamma p(t))$ coordinates. The largest Lyapunov exponent Λ follows

$$\Lambda = \lim_{t\to\infty} \frac{1}{t} \ln \frac{\|w(t)\|}{\|w(0)\|}. \tag{27}$$

In Fig. 3 we show the Lyapunov time $T_\Lambda = 1/\Lambda$ versus energy densities h for given $E_J = 1$. It matches well with the analytical results obtained in [5].

[1] C. Skokos, D. O. Krimer, S. Komineas, and S. Flach, "Delocalization of wave packets in disordered nonlinear chains," Phys. Rev. E **79**, 056211 (2009).

[2] P. Richard, "Feynman. statistical Mechanics, a set of lectures," Frontiers in Physics. Perseus Books (1972).

[3] S. Chakravarty and S. Kivelson, "Photoinduced macroscopic quantum tunneling," Phys. Rev. B **32**, 76 (1985).

[4] M. Kac, G. Uhlenbeck, and P. Hemmer, "On the van der Waals Theory of the Vapor-Liquid Equilibrium. i. Discussion of a One-Dimensional Model," Journal of Mathematical Physics **4**, 216 (1963).

[5] L. Casetti, C. Clementi, and M. Pettini, "Riemannian theory of Hamiltonian chaos and Lyapunov exponents," Phys. Rev. E **54**, 5969 (1996).